**Proceedings of ASME Turbo Expo 2017: Turbomachinery Technical Conference and Exposition**
**GT2017**
**June 26-30, 2017, Charlotte, NC, USA**

# GT2017-63010

# ASSESSMENT OF BEARING HEAT GENERATION PREDICTION BY THE PROGRAM ADORE WITH RESPECT TO EXPERIMENTAL RESULTS AND SHABERTH PREDICTIONS

**Brian D. Nicholson, Garry D. Givan, Kevin L. Thompson, Capt. Justin Mason**
Air Force Research Laboratory
Wright-Patterson AFB, Ohio, USA

**Pradeep K. Gupta**
PKG, Inc.
Clifton Park, NY, USA

**Hitesh K. Trivedi**
UES, Inc.
Dayton, Ohio, USA

## ABSTRACT

This work details the heat generation analysis of a turbine aero-engine main-shaft bearing using the computer program Advanced Dynamics Of Rolling Elements (ADORE). The empirical models used for traction and churning heat generation are detailed. The predictions of ADORE are shown to demonstrate the differing contributions of traction and churning to total heat generation at different load/speed regimes. These results are then compared with experimental results. In addition, the results of ADORE are also compared with results from the well-known bearing analysis program SHABERTH (Shaft Bearing Thermal Analysis). The comparisons showed good agreement between ADORE and the experimental results for loads between 13.35 and 53.40 kN and speeds between 1.8 and 2.2 MDN. The results also showed under prediction of heat generation by SHABERTH in this regime. Limitations of both programs were identified and speculated to include limitations in the empirical models due to the lack of available experimental traction data at high speeds/loads. Finally, recommendations for future research are provided which will likely provide significant improvements in the ability to predict bearing heat generation in turbine aero-engine applications.

## NOMENCLATURE

**Capital Letters**

| | |
|---|---|
| $A$ | Exposed frontal area, effective surface area ($m^2$) |
| AISI | American Iron and Steel Institute |
| AMS | Aerospace Material Specification |
| $C_D$ | Tabulated drag coefficient |
| $C_n$ | Flow coefficient |
| $C_p$ | Specific heat (J/kg°C) |
| DN | Bearing bore diameter in mm × shaft speed in rpm |
| MDN | Million DN |
| $F_D$ | Drag force on rolling element (N) |
| $K$ | Thermal conductivity (W/m/°K) |
| $M$ | Bearing torque (N·m) |
| $M_C$ | Moment on cylindrical surface (N·m) |
| $M_e$ | Moment on end surface (N·m) |
| $Q_O$ | Power loss transferred to the lubricant (kW) |
| $Q_T$ | Total bearing power loss from torque meter (kW) |
| $Q_{TO}$ | Total power loss determined from $Q_O$ (kW) |
| $R^2$ | Coefficient of determination |
| $R_e$ | Reynolds number |
| $T$ | Lubricant temperature (°C) |
| $T_a$ | Taylors number |
| $T_{in}$ | Lubricant inlet temperature (°C) |
| $T_o$ | Reference lubricant temperature (°C) |
| $T_{out}$ | Lubricant outlet temperature (°C) |
| $U$ | Surface velocity (m/s) |
| $V$ | Velocity (m/s) |
| XCAV | Lubricant volume percentage (SHABERTH input parameter) |

**Lower Case Letters**

| | |
|---|---|
| $b_i$ | Power loss correlation coefficient |
| $c$ | Operating clearance (m) |
| $d$ | Diameter of rolling element (m) |
| $f$ | Friction factor |
| $f_L$ | Laminar flow factor |
| $\dot{m}$ | Lubricant mass flow rate (kg/s) |
| $p$ | Pressure (Pa) |

Approved for public release, case number 88ABW-2016-5230; distribution is unlimited.

| | |
|---|---|
| $q$ | Bulk heating (kW) |
| $r$ | Element radius (m) |
| $r_{in}$ | Inner radius (m) |
| $r_{out}$ | Outer radius (m) |
| $s$ | Strain rate |
| $u$ | Relative velocity (m/s) |
| $z$ | Coordinate through film thickness (m) |

**Greek Symbols**

| | |
|---|---|
| $\alpha$ | Pressure-Viscosity coefficient (1/Pa) |
| $\alpha^*$ | Constitutive pressure-viscosity constant (1/GPa) |
| $\beta$ | Temperature-Viscosity coefficient (1/°K) |
| $\beta^*$ | Constitutive temperature-viscosity constant (1/°K) |
| $\mu$ | Dynamic viscosity (Pa·s) |
| $\mu_0^*$ | Reference dynamic viscosity (Pa·s) |
| $\nu$ | Lubricant kinematic viscosity ($m^2/s$) |
| $\rho$ | Lubricant density, effective lubricant density ($kg/m^3$) |
| $\tau$ | Shear stress (Pa) |
| $\Phi_D$ | Empirical adjustment factor |
| $\omega$ | Shaft speed, angular velocity (rad/s) |

## INTRODUCTION

As modern manned turbine aero-engines evolve, ever increasing thermal management challenges are placed on the engine designers. Thermal management capacity is a key factor in limiting aircraft payload [1]. This is due to the fact that the aircraft fuel supply is the main heat sink for the majority of systems on the aircraft yet it is limited by a maximum safe useable temperature [2, 3]. Heat loads to the fuel consist of the engine and its subsystems as well as a growing number of avionics, sensors, and other electronic systems [1-5]. With respect to engine mechanical systems, the engine oil functions partially to lubricate the bearings, but mostly as the bearing coolant [6, 7]. Typically, the oil system expels its heat through a fuel cooled oil cooler, occasionally with a supplemental air cooled oil cooler [2, 5]. Due to the system level thermal challenge, accurate prediction of bearing heat generation is of significant importance. While computational fluid dynamics, Finite Element Analysis, and numerical elastohydrodynamic lubrication computations will likely be the methods of prediction in the future, they are currently much too expensive in computational time to be practical in the bearing design process [7]. Therefore, current state-of-the-art bearing analysis programs rely on empirical models for the different heat generation phenomena [8].

Frictional dissipation at the contacts between various bearing elements as well as churning and drag effects associated with circulating lubricants constitute the main sources of heat generation in typical turbine engine rolling bearings. While the high speed sliding contacts at rolling element to cage and cage to race contacts can be reasonably modeled by experimentally determined constant friction coefficients, modeling of rolling-sliding contacts between the rolling elements and race has been a subject of considerable interest over several decades. Due to the vast amount of published work on this subject, a fair review

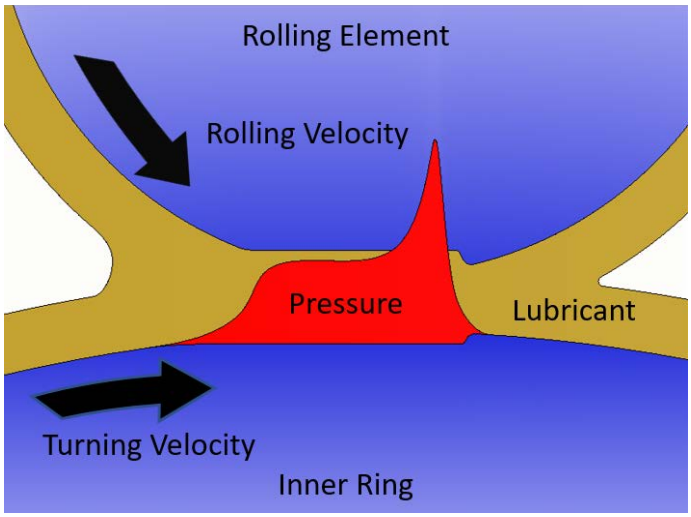


**Figure 1. ELASTOHYDRODYNAMIC CONTACT**

of the available literature is beyond the scope of this investigation. Predictions of lubricant film thickness and modeling of traction in elastohydrodynamic contacts continue to be subjects of extreme practical significance. While current simple algebraic equations derived from numerical solutions to the Reynolds equation of fluid flow through the elastohydrodynamic contacts are well established as reliable tools to compute lubricant film thickness in a concentrated contact, reliable traction predictions remain in developing stages primarily due to complex behavior of the lubricants in the high pressure rolling-sliding contacts. Since measurement of the constitutive constants of the lubricants continues to be an extremely difficult and complex task, the general approach has been to experimentally measure traction and back fit the experimental data to hypothetically formulated rheological models to derive the applicable constitutive constants by simple regression analysis. Perhaps, the simplest traction model based on such an approach is due to Kannel and Walowit [9], who have presented a simple analytical formulation based on Newtonian flow of lubricants. The model yields a rather simple relation to define traction coefficient as a function of slip rate, the applicable elastohydrodynamic contact parameters, and the estimated constitutive constants for the prescribed lubricants. Realistic implementation of the model to a rolling bearing requires both an accurate simulation of slip velocity in the rolling-sliding contact and experimental traction data that closely replicates the modeled conditions. Current real-time dynamics models, such as ADORE [8], present significant advancement in simulation of slip velocity over simpler, quasi-static based bearing performance simulation codes. However, current experimental traction rigs are incapable of replicating the very high contact pressure and rolling velocity of modern turbine engine bearing applications. Thus, traction data is generally obtained at highest permissible rolling velocity and the derived constitutive constants are used over the entire applicable operating conditions. As the actual operating conditions move farther from the limits of experimental data, the model results in greater uncertainty in traction predictions.

As a further advancement of a traction model for high pressure concentrated contacts, Johnson and Tevaarwerk [10] postulated a visco-elastic model where the fluid is basically modeled as an elastic solid under high pressure where the Newtonian model provides an unrealistically high viscosity. Subsequent to this work, Bair and Winer [11] developed further refinements to modeling the visco-elastic behavior. Gupta [12] has implemented both the works of Johnson and Tevaarwerk [10] and Bair and Winer [11] in the bearing dynamics code ADORE to model the traction behavior of the MIL-L-7808 type lubricant in turbine engine bearings. More recently, Bair [13, 14] has presented experimentally validated "shear thinning" traction models, where the effective lubricant viscosity is dependent on shear stress. These models are analytically more complex; thus the implementation of these models in bearing performance simulation tools has yet to be undertaken.

Since the slip velocities in rolling bearing contacts constantly change as the rolling elements continue to collide back and forth in the cage pockets as they move along the rolling track, a realistic simulation of these velocities requires a real-time integration of the classical equations of motion of rolling elements. Therefore, quasi-static bearing performance modeling tools, such as SHABERTH [15, 16] may not be adequate for simulation of slip velocities in rolling bearing contacts. ADORE [8] provides a fairly generalized integration of the differential equations of motion and implements both Newtonian and visco-elastic traction models. Although ADORE is the baseline model used in the present investigation, there are a number of other available dynamics models for rolling bearing performance simulation. Gupta [17] has recently presented a fairly detailed review of available rolling bearing performance modeling tools.

Modeling of realistic flow of the circulating lubricant and the resulting churning and drag effects in rolling bearings is indeed a very difficult task. In spite of significant advancement in computational fluid dynamics methods, these more complex techniques have not yet provided any improvements in modeling churning and drag effects over the simple relations, based on classical laminar and turbulent flow, as presented by Rumbarger et al [18] several decades ago. Thus, simulation of these effects in ADORE is still limited to these simple relations, although some refinements to the empirical drag coefficients have been made. It should be pointed out that since only the nominal rolling element velocities enter in the classical flow equations, subtle variations in bearing element velocities do not affect the churning and drag effects. Thus, modeling of bearing heat generation resulting from these effects is equally good with both dynamic and quasi-static bearing performance tools.

Primarily due to the amount of lubricant circulating in the bearing cavity, a significant fraction of bearing heat generation in turbine engine bearings, under a wide range of operating conditions, is due to churning and drag effects. Therefore, both the dynamic and quasi-static bearing performance modeling tools may provide equally acceptable predictions of bearing heat generation. In some of the modern turbine engine applications; however, where the applied loads are significantly more severe, the overall heat generation due to frictional dissipations becomes comparable to the churning and drag contribution. Under these conditions, the role of traction models become important. Therefore, the dynamic models may provide improved overall heat generation simulation.

The primary objective of the present investigation is to segment bearing heat generation into traction and lubricant churning/drag effects and evaluate ADORE predictions against recent experimental data obtained by Forster et al [19] for a typical high-speed turbine engine main-shaft bearing. After a brief review of the modeling fundamentals and the experimental procedure, the predicted bearing heat generation data is presented in terms of the traction and lubricant drag fractions. Conditions under which the traction effects become significant are then identified. Overall bearing heat generation, as predicted by ADORE, are then compared to the experimental data to establish the model strengths and identify the regions where further model refinements are necessary.

## ADORE HEAT GENERATION

### Traction Model

Modeling of traction in elastohydrodynamic contacts basically consists of two parts: computation of lubricant film thickness based on ambient pressure and temperature properties of the lubricant and computation of traction, which requires modeling of lubricant rheology in the high pressure concentrated contact. For the present investigation, the film thickness under isothermal conditions is first computed by the well-established point contact film thickness formula presented by Hamrock and Dowson [20], and then corrected for thermal effects by applicable film thickness reduction factors [21-23]. The widely used Newtonian model [8, 9], based on constitutive constants derived from experimental traction data, is used for the computation of traction. The model basically consists of the following fundamental formulation:

Energy Equation:

$$K\frac{\partial^2 T}{\partial z^2} = -\tau s \tag{1}$$

Geometric Compatibility:

$$\frac{\partial u}{\partial z} = s(\tau, p, T) \tag{2}$$

And Constitutive Relation:

$$s(\tau, p, T) = \frac{\tau}{\mu(p,T)} \tag{3}$$

**Table 1. CONSTITUTIVE CONSTANTS FOR MIL-PRF-23699 FOR TRACTION MODELING**

| | |
|---|---|
| Reference Temperature (°K) | 394 |
| Reference Viscosity, $\mu_0^*$ (Pa·s) | $3.428\times10^{-3}$ |
| Pressure-Viscosity Constant, $\alpha^*$ (1/GPa) | $5.802\times10^{-9}$ |
| Temperature-Viscosity Constant, $\beta^*$ (1/°K) | $4.512\times10^{-2}$ |

where $K$ is the thermal conductivity, $T$ is the temperature, $z$ is the coordinate through the film, $u$ is the relative velocity, $s$ is the strain rate, $p$ is the pressure, $\tau$ is the shear stress, and $\mu$ is the viscosity. The viscosity-pressure-temperature relation, applicable in the high pressure contact takes the form:

$$\mu = \mu_0^* e^{\alpha^* p + \beta^*(T_0 - T)} \tag{4}$$

where $\mu_0^*$ is the reference viscosity and $\alpha^*$ and $\beta^*$ are respectively the viscosity-pressure and viscosity-temperature constants.

Equations (1) through (4) are essentially solved simultaneously to compute the traction-slip relation at applicable operating conditions. The constitutive constants in equation (4) are derived by regression analysis of available traction data. The constants for the current lubricant are summarized in Table 1.

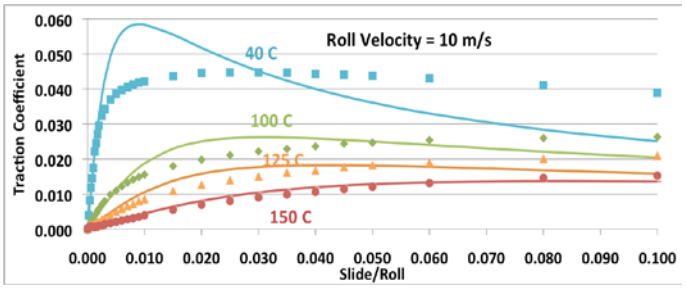


**Figure 2. TRACTION MODEL CORRELATIONS (SOLID LINE) AND EXPERIMENTAL RESULTS (POINT) AT A CONSTANT PRESSURE OF 2 GPa AND ROLLING VELOCITY OF 10 m/s**

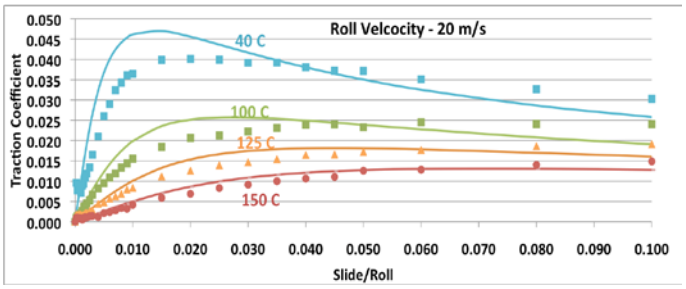


**Figure 3. TRACTION MODEL CORRELATIONS (SOLID LINE) AND EXPERIMENTAL RESULTS (POINT) AT A CONSTANT PRESSURE OF 2 GPa AND ROLLING VELOCITY OF 20 m/s**

Typical model correlations against the experimental data (obtained by traction testing in this work) are shown in Figure 2 and Figure 3 at the contact stress of 2 GPa and rolling velocities of 10 and 20 m/s respectively.

As the temperature increases and the effective viscosity decreases, the correlation with experimental data gets progressively better. As described above the operating temperature of the test bearing was 121 °C, therefore, the model predictions are fairly good at the indicated contact pressure and rolling velocities. Although the maximum contact pressure in the test bearing was 2 GPa, the rolling velocities varied in the range of about 60 to 90 m/s, which are far beyond the range of available traction data. Thus, application of the traction model under such high speed conditions results in significant extrapolation and there may be uncertainties in traction predictions. The applicable traction curves predicted for bearing test conditions, as derived by above constitutive constants, are shown in Figure 4 and Figure 5 under the lower and higher ends of rolling velocities.

As the contact pressure and rolling velocities increase, the computed traction coefficient tends to develop a sharp peak at low slip velocities and a very rapid fall off with increasing slip velocities as shown in Figure 4 and especially Figure 5. Some slight fall off in traction with increasing slip is seen in the experimental traction data shown in

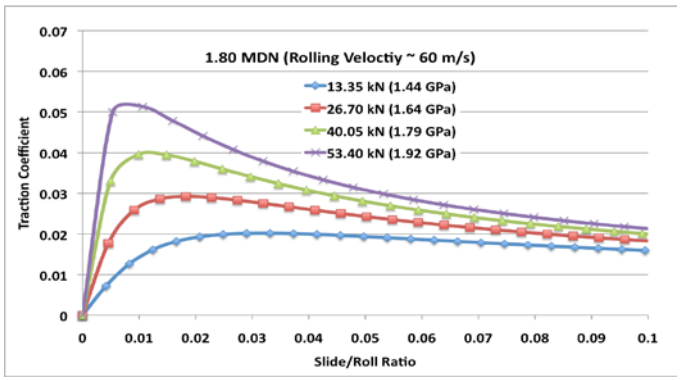


**Figure 4. ADORE SIMULATED TRACTION/SLIP AS A FUNCTION OF CONTACT PRESSURE AT 1.80 MDN at 121 °C**

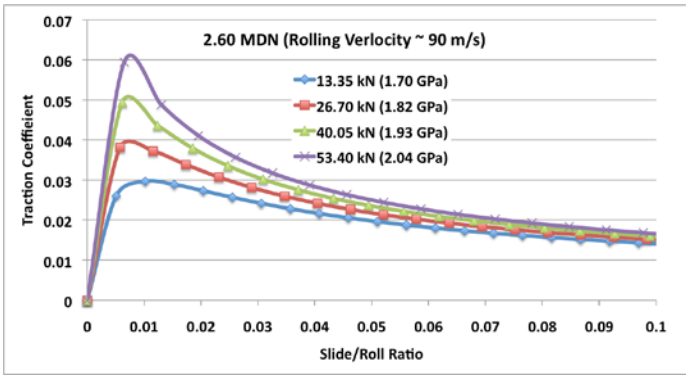


**Figure 5. ADORE SIMULATED TRACTION/SLIP AS A FUNCTION OF CONTACT PRESSURE AT 2.60 MDN at 121 °C**

Figure 2 and Figure 3 and may be justified in terms of thermal effects in the contact, but the increasing steep slope and the large fall off with increasing rolling velocities and contact pressures has yet to be validated. Unfortunately, current traction rigs are limited to a maximum rolling velocity in the range of 20 to 25 m/s. Thus the traction predictions at high loads and high rolling velocities may be no more than speculation at this point in time. When the traction contribution in overall bearing heat generation is significant, then there may be uncertainties in heat generation predictions under such extreme conditions.

Although there is no presently available experimental traction data at the very high rolling velocities typical of modern turbine engine bearing applications, preliminary traction models based on visco-elastic and shear-thinning effects have shown significantly different traction behavior in comparison to the Newtonian model [8, 10–14]. Due to both analytical and related numerical complications, implementation of these models, for the current lubricant, in bearing dynamics performance simulation tools, such as ADORE, is indeed a major undertaking. For the present, however, model predictions are restricted to the available Newtonian traction model.

## Churning and Drag Models

Churning and drag models in most bearing performance simulation tools are still based on the simple formulation developed by Rumbarger et al [18] several decades ago. The drag force on the rolling elements is simply written as:

$$F_D = \frac{1}{2}\Phi_D C_D \rho V^2 A \tag{5}$$

where $\rho$ is the effective lubricant density, $V$ is the velocity, $A$ is the exposed frontal area, $\Phi_D$ is an empirical adjustment factor, and $C_D$ is a tabulated drag coefficient as a function of Reynolds number:

$$R_e = \frac{\rho V d}{\mu} \tag{6}$$

where $d$ is the diameter of the rolling element and $\mu$ is the lubricant viscosity.

Since the bearing cavity is never completely filled with the lubricant, the empirical adjustment factor, $\Phi_D$, simply adjusts the applicable density. Based on experimental experience of the authors, a value of 0.050 has been typically used for many applications. Thus, for consistency, $\Phi_D$ is set as 0.050 in the present investigation.

Churning moments are based on flow around cylindrical elements. The moments are computed both on cylindrical and end surfaces of a cylinder. The moment on the cylindrical surface is written as:

$$M_C = \left(\frac{1}{2} f \rho U^2\right) Ar \tag{7}$$

where $U$ is the surface velocity, $A$ is the effective surface area and $r$ is the radius. The friction factor, $f$, depends on the type of flow, primarily determined by the speed, as defined below.

Vortex Turbulent Flow:

$$\frac{f}{f_L} = 1.3\left(\frac{T_a}{41}\right)^{0.539474} \tag{8a}$$

Where Taylors Number:

$$T_a = \frac{\rho r \omega c}{\mu}\sqrt{\frac{c}{r}} > 41 \tag{8b}$$

Couette Turbulent Flow:

$$\frac{f}{f_L} = 3.0\left(\frac{R_e}{25000}\right)^{0.85596} \tag{8c}$$

Where Reynolds Number:

$$R_e = \frac{\rho r \omega c}{\mu} > 25000 \tag{8d}$$

The laminar flow factor:

$$f_L = \frac{16}{R_e}, \quad R_e < 25000 \text{ or } T_a < 41 \tag{8e}$$

where $\omega$ is the angular velocity and $c$ is the operating clearance.

For computing the moment on the end surfaces of a cylindrical element, the churning moment is defined as:

$$M_e = \frac{1}{2} C_n \rho \omega^2 r^5 \tag{9}$$

where the coefficient $C_n$ is based on type of flow defined by the Reynolds number ($R_e = \frac{\rho \omega r^2}{\mu}$):

Laminar flow ($R_e$ < 300,000):

$$C_n = \frac{3.87}{R_e^{0.50}} \text{ and } r^5 = r_{out}(r_{out}^4 - r_{in}^4) \tag{10a}$$

Turbulent flow (Re > 300,000):

$$C_n = \frac{0.146}{R_e^{0.20}} \text{ and } r^5 = r_{out}^{0.40}(r_{out}^{4.60} - r_{in}^{4.60}) \tag{10b}$$

where $r_{out}$ and $r_{in}$ are respectively the outer and inner radii, and the Reynolds number is based on the outer radius.

For a ball, although no straightforward expressions are available, if the loss is approximated as that occurring on a projected area on a plane normal to the ball angular velocity vector, then the ball can represented by a thin disk and the above expressions may be used for computing the churning moment.

## EXPERIMENTAL PROCEDURE

### Test Rig

Figure 6 displays the test rig used to obtain the experimental data. The rig uses a 75 kW motor which drives a hollow shaft supported by two 133-mm bore angular contact ball bearings. A hydraulic piston is used to provide a desired thrust load to the bearings, which become loaded against each other. Under race lubrication is provided to the bearings with an oil jet to the interior of the shaft. Grooves on the interior wall of the shaft distribute the oil to each bearing. The oil is scavenged from three ports at bottom dead center, with 1 port on each side of each bearing. A thermocouple is located at the oil jet exit to indicate oil inlet temperature, while thermocouples in the scavenge line, near the test head provide outlet temperature. Additionally, bearing outer race temperatures are monitored through thermocouples mounted to the outer ring at the 6 and 12 o'clock positions.

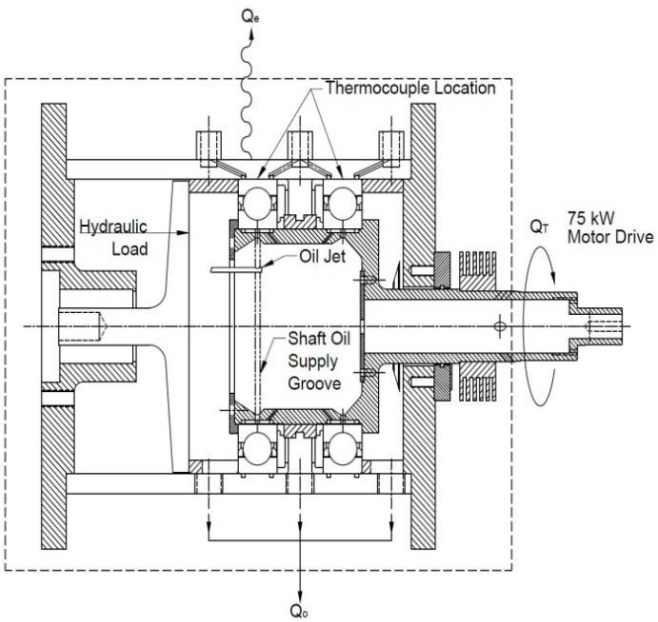


**Figure 6. EXPERIMENTAL TEST RIG CONFIGURATION**

**Table 2. TEST BEARING NOMINAL GEOMETRY**

| | |
|---|---|
| Bore Diameter (mm) | 133.35 |
| Outside Diameter (mm) | 202 |
| Pitch Diameter (mm) | 168 |
| Ball Diameter (mm) | 22.2 |
| Contact Angle (º) | 28 |
| Number of Balls | 20 |

### Test Bearing

The two test bearings are comprised of M50 NiL races (an outer ring and a split inner ring each), heat-treated in compliance with Aerospace Material Specification (AMS) 6278C, twenty (20) AISI M50 rolling elements each heat-treated to AMS 6491C, and AISI 4340 cages, heat treated to AMS 6414 and silver plated in accordance with AMS 2410J. The oil delivery paths (shown in Figure 7) consist of 1.59-mm diameter passages to the cage land of each side of the inner race and a 3.81 by 1.27-mm passage in the unloaded inner ring which provides lubrication to the balls and race. The two cage land lube passages and the race passage occur at sixteen locations, equally spaced around the circumference of the inner ring. The nominal geometry of the bearing is shown in Table 2.

### Lubricant

The lubricant used during testing was an experimental polyolester in development for high-performance engines. The design objectives for the developmental lubricant are to improve gear load capacity and compatibility with fluoro-elastomer o-rings, while maintaining the thermal stability of the high-thermal-stability MIL-PRF-23699 lubricants.

Properties of the lubricant are representative of qualified type II (MIL-PRF-23699) aircraft engine lubricants. Lubricant density (kg/m$^3$) and specific heat (J/kg°C) as a function of temperature were empirically determined and are shown in Equations (11) and (12) respectively.

$$\rho = 1 \times 10^3(-7.296 \times 10^{-4}T + 1.009) \quad (11)$$

$$C_p = 2.4171T + 1763.2 \quad (12)$$

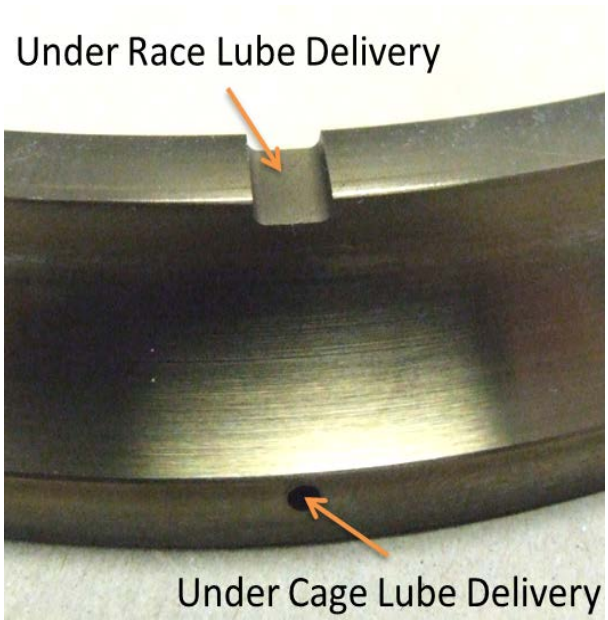


**Figure 7. LUBRICANTION DELIVERY PASSAGES ON UNLOADED SIDE OF BEARING INNER RACE**

**Table 3. PROPERTIES OF MIL-PRF-23699 AT AMBIENT PRESSURE CONDITIONS**

| | |
|---|---|
| Density, $\rho$ (kg/m$^3$) | 903.345 |
| Thermal Conductivity, $K$ (W/m/°K) | 0.1426 |
| Reference Temperature, $T_o$ (°K) | 394 |
| Reference Dynamic Viscosity, $\mu_0^*$ (Pa·s) | $3.428 \times 10^{-3}$ |
| Pressure-Viscosity Coefficient, $\alpha$ (1/Pa) | $1.0396 \times 10^{-8}$ |
| Temperature-Viscosity Coefficient, $\beta$ (1/°K) | 2559.3 |

Lubricant kinematic viscosity was fitted to Walther's temperature-viscosity equations as described by Wright [24]. Kinematic viscosity (m$^2$/s) is shown in Equation (13), where $a$ = 9.102 and $m$ = 3.586. Dynamic viscosity (Pa·s) can be described as shown in Equation (14), where $\mu_o$, $T_o$, $\alpha$, $\beta$, and other lubricant properties may be seen in Table 3.

$$\nu = 1 \times 10^{-6}\left\{\log^{-1}\left[\log^{-1}(a - m\log T)\right] - 0.7\right\} \quad (13)$$

$$\mu = \mu_o e^{\left[\alpha p + \beta\left(T^{-1} - T_o^{-1}\right)\right]} \quad (14)$$

## Test Procedure

A matrix of 398 test conditions was constructed in two phases; low-speed and high-speed. Low-speed testing ranged from 1.5 MDN to 2.0 MDN in increments of 0.1 MDN. These speeds correspond to the general range of low pressure spool speeds in manned aero-engines. Thrust loading was applied from 13,350 to 53,400 N in increments of 13,350 N. These loads result in Hertzian contact stresses from 1.25 to 1.95 GPa on the inner race and 1.35 to 2.00 GPa on the outer race as calculated by ADORE. Oil delivery temperatures were 66, 93, and 121 °C, while flow rates were 9.4 and 11.4 L/min per bearing. These parameters were controlled within 20 rpm, 22 N, 1 °C, and 0.20 L/min per bearing respectively.

High-speed testing was conducted at speeds from 2.0 to 2.6 MDN in increments of 0.1 MDN. Flow rates were supplied at 7.3, 9.4, and 11.4 L/min. Thrust loading and oil delivery temperatures were identical to those used in low-speed testing.

During low-speed testing, an in-line rotating strain-gauge torque sensor was used to determine the total power loss via Equation (15), where $M$ is the measured bearing torque in Nm and $\omega$ is the shaft speed in rad/s.

$$Q_T = M\omega/1{,}000 \quad (15)$$

While some of the power loss occurs as heat transfer to the surrounding structure and environment, the majority of the power loss is accounted for as heat transfer to the oil as calculated in Equation (16), where $\dot{m}$ is the mass flow rate in kg/s, $C_p$ is the oil specific heat in J/kg°C, and $T_{in}$ and $T_{out}$ are the oil inlet and outlet temperatures respectively in °C.

$$Q_O = \dot{m}C_p(T_{out} - T_{in})/1{,}000 \quad (16)$$

During high-speed testing, the torque sensor was not used due to speed limitations, and instead, the total power loss was correlated to the heat transfer into the oil and the oil outlet temperature using the data from low-speed testing. The correlated total power loss is given in Equation (17), where $b_1$ = 1.202, $b_2$ = 1.118, and $b_3 = -5.94 \times 10^{-3}$.

$$Q_{TO} = b_1 + b_2 Q_O + b_3 T_{out} \quad (17)$$

The correlation coefficient from the data regression showed a superb fit of $R^2$ = 0.998. Selected results of the testing may be seen in the following section. Complete results may be found as published by Forster et al [19].

## COMPARISONS OF HEAT GENERATION

Using the previously discussed traction and lubricant churning and drag models, the bearing dynamics code, ADORE was used to compute bearing heat generation for the 133-mm angular-contact ball bearing described previously. Forster et al [19] has documented a significant amount of experimental data. The published data includes experimentally measured bearing heat generation at several values of applied thrust load and at several operating speeds in the range of 1.6 to 2.6 MDN as detailed in the experimental procedure section.

Since in most turbine engine applications, most of the power loss is generally attributed to churning and drag effects, the first step was to identify significance of the traction model effects, if any, in comparison to the churning and drag losses. Thus, the fraction of total power loss resulting from churning/drag, as predicted by ADORE, is plotted in Figure 8. It is noted that while at light loads over 90% of the total bearing heat generation comes from the churning/drag effect, the traction model effects are quite comparable with the churning/drag contribution at high loads as shown in Figure 10. Thus, a realistic traction model does play an important role in modeling total bearing power loss.

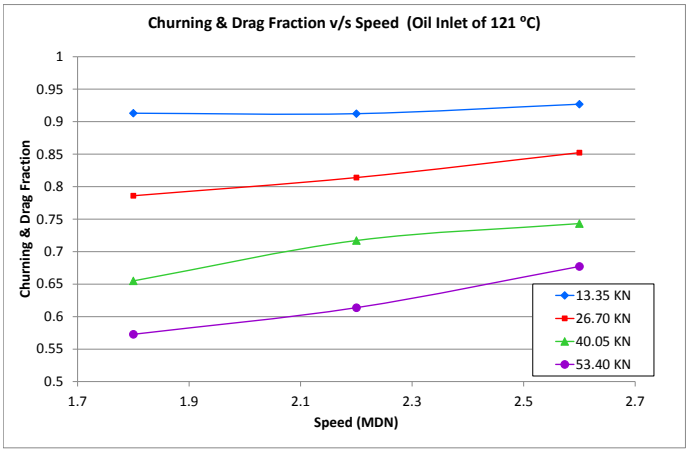


**Figure 8. ADORE RATIO OF CHURNING AND DRAG CONTRIBUTION TO THE TOTAL BEARING POWER LOSS AS A FUNCTION OF APPLIED LOAD AND SPEED**

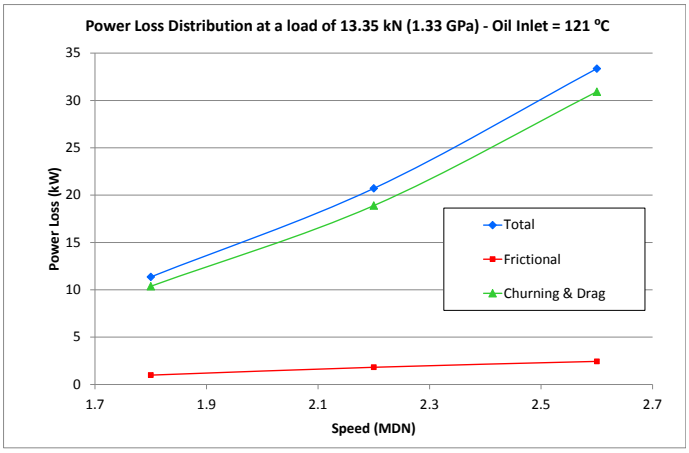


**Figure 9. ADORE POWER LOSS DISTRIBUTION AT A THRUST LOAD OF 13.35 kN**

Of the total predicted power loss, the actual distribution in terms of traction and churning/drag contributions are shown at light and heavy loads in Figure 9 and Figure 10 respectively.

Total bearing power loss measured experimentally is shown against ADORE predictions as a function of speed and load in Figure 11.

Note that ADORE predictions agree very well (relative error between 2 to 10 %) with experimental data except at very high speeds, where ADORE is over predicting the power loss (relative error of nearly 30%). The existence of non-Newtonian behavior of lubricant in the contact zone is a well-known feature of EHL (Elastohydrodynamic Lubrication) in the field of Tribology. Hence, this discrepancy is partially, if not completely, coming from the limitation of Newtonian traction model predictions at high rolling speeds as discussed earlier. At high loads and speeds the Newtonian traction model predicts a rather high traction slope, as illustrated in Figure 4 and Figure 5. This is controversial, since no experimental traction data is available to support such a behavior. The prediction of traction coefficients under such

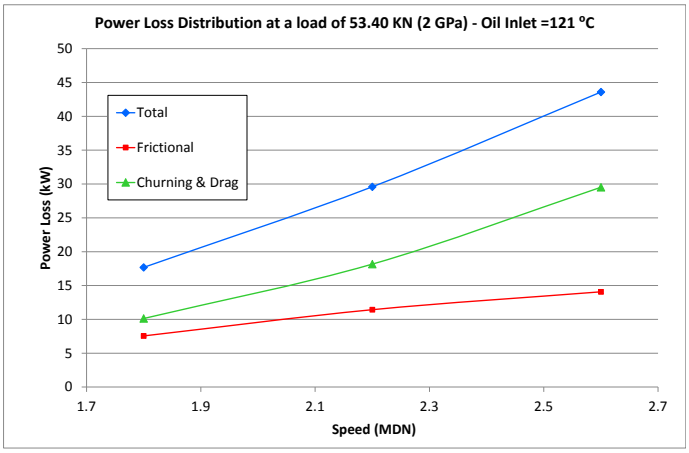


**Figure 10. ADORE POWER LOSS DISTRIBUTION AT A THRUST LOAD OF 53.40 kN LOAD OF 53.30 kN**

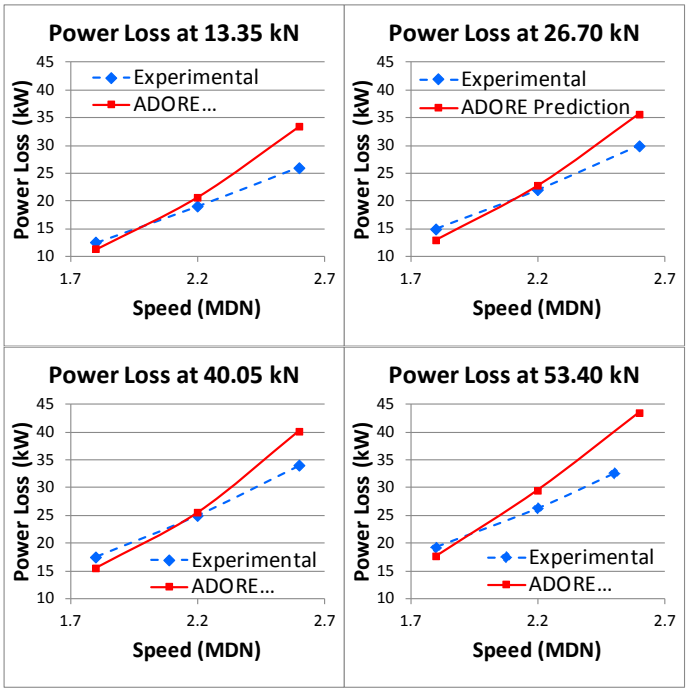


**Figure 11. ADORE PREDICTIONS AGAINST EXPERIMENTALLY MEASURED POWER LOSS AS A FUNCTION OF SPEED AND APPLIED LOAD (Note: An experimental data point for 53.4 kN and 2.6 MDN was not obtained. 2.5 MDN was used instead)**

conditions may be much higher than the true value. This leads to high power loss predictions as seen in Figure 11. This agreement is expected to improve with the implementation of visco-elastic and shear-thinning type traction models in future work. The degree of that agreement will provide insight into the extent of the effect of the non-Newtonian lubricant behavior on the power loss.

Forster et al [19] have also shown the predictions made by the popular quasi-static bearing code, SHABERTH. Since, in quasi-static analysis, the slip in the ball/race contact is not only constant, but also an estimate based on a kinematic hypothesis which is insensitive to applied load, SHABERTH power loss predictions are not expected to show any load dependence. This is what is seen in Figure 12, where both the ADORE and SHABERTH predictions are shown as a function of applied load at a given operating speed; the SHABERTH predictions are reproduced from the Forster et al [19] publication. While SHABERTH predictions are load independent, the load dependence seen in the ADORE predictions agree well (<10% relative error) with the experimental data. This is primarily due to more realistic modeling of traction effects as a function of load in ADORE.

All of the above data corresponds to oil inlet temperature of 121 °C. At a lower temperature of 66 °C, when the lubricant film thickness is much higher, the Newtonian traction predictions are much higher in comparison to experimental data. Thus, under

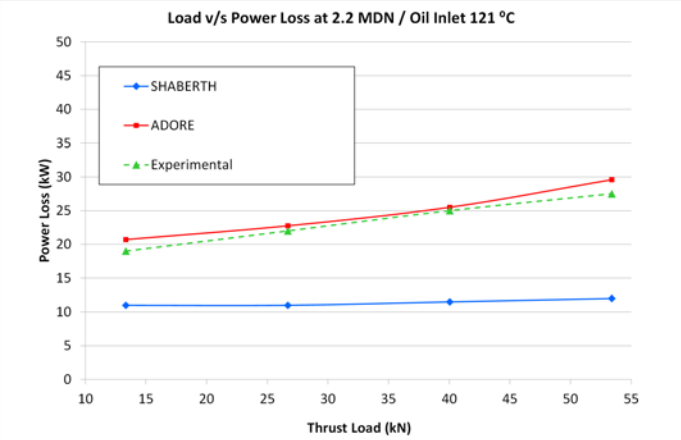


**Figure 12. ADORE AND SHABERTH PREDICTIONS OF BEARING POWER LOSS AGAINST EXPERIMENTAL DATA**

such conditions the power loss predictions are expected to be higher than the experimental data. This is what is seen in Figure 13, where the power loss is plotted as a function of speed. For comparison, SHABERTH predictions as reported by Forster et al [19], are also shown. The overall pattern of the variation is similar. In fact, if the empirical drag coefficients are adjusted, both ADORE and SHABERTH will provide similar predictions as a function of speed. It should be noted that with respect to SHABERTH, the lubricant volume percentage (XCAV) was calculated using Parker's formulation [25]. This parameter is significant in SHABERTH's prediction of churning. Pinel et al. [26] identified limitations to Parker's formulation with respect to mode of lubricant delivery. This may be at play here as well since Parker's experiments used jet lubrication while this is an under-race lubricated bearing. While this would only account for a portion of the underprediction shown in Figure 12, it could account for the majority of the difference shown in Figure 13.

## CONCLUSIONS

Based on the comparison of bearing heat generation, as predicted by the bearing dynamics code ADORE, with the published experimental data of a turbine engine ball bearing, the following conclusions may be reached:

1. While at light loads the majority of bearing power loss is due to lubricant churning and drag effects, traction contributions become equally significant at high loads.

2. At low to moderate applied loads and speeds, ADORE predictions agree fairly well with the available experimental data.

3. At high loads, when the traction contribution to overall bearing power loss is significant, the current Newtonian traction model in ADORE predicts a somewhat higher power loss in comparison to the experimental data.

4. The load dependence of experimental bearing power loss is in agreement with ADORE predictions.

5. Unlike the dynamics code ADORE, since quasi-static bearing models such SHABERTH simply compute slip velocities from certain kinematic hypotheses, no load dependence of bearing power loss can be computed with these models.

6. Under operating conditions when the majority of bearing heat generation is due to lubricant churning and drag (i.e. Newtonian lubricant behavioral regime), the predictions of both dynamic and quasi-static bearing performance tools will be in agreement with experimental data assuming proper consideration to drag coefficients.

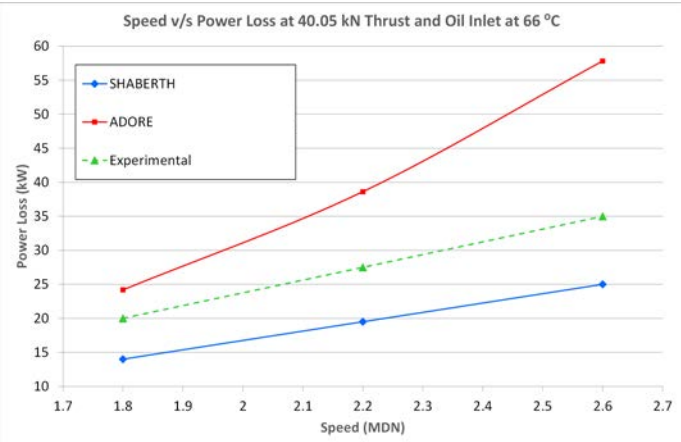


**Figure 13. ADORE AND SHABERTH PREDICTIONS OF BEARING POWER LOSS AS A FUNCTION OF SPEED AT LOWER OIL TEMPERATURES OF 66 °C (as opposed to 121 °C)**

## RECOMMENDATIONS FOR FUTURE DEVELOPMENTS

Significant improvements in elastohydrodynamic traction models at high contact pressures and rolling bearings are essential for improved predictions of heat generation in turbine engine bearings. The application of currently used Newtonian traction models, which were essentially developed from regression analysis of experimental traction data obtained under low rolling velocities, is limited. A more rigorous validation and implementation of more advanced traction models based on visco-elastic and shear-thinning effects may have a significant contribution to improved bearing heat generation modeling. In addition to the related analytical modeling, further advancements of experimental traction rigs are essential for the development of realistic traction models at the very high loads and speeds typical of modern turbine engine bearing applications.

## ACKNOWLEDGMENTS

The research reported herein was sponsored by the United States Air Force (USAF) under the Small Business Innovation Research (SBIR) Phase I contract, FA8650-13-M-2406, awarded to Pradeep K Gupta, Inc. (PKG, Inc.). The Project Engineer was Capt. Justin Mason. The experimental work was conducted by UES Inc under USAF Contract FA8650-07-D-2804 and by the Air Force Research Laboratory (AFRL), Wright-Patterson Air

Force Base, Ohio. The Project Engineer was Mr. Garry D. Givan. Special thanks to Dr. Lewis Rosado, AFRL/RQTM by whose leave this paper was written and presented. The authors would also like to thank the conference paper reviewers, whose criticism and guidance led to improvements in this paper.

## REFERENCES

[1] Mahefkey, T., Yerkes, K., Donovan, B., and Ramalingam, M., 2004, "Thermal Management Challenges for Future Military Aircraft Power Systems," SAE, Power Systems Conference, Reno, Nevada.

[2] Harrison, W. E., Binns, K, E., Anderson, S. D., and Morris, R. W., 1993, "High Heat Sink Fuels for Improved Aircraft Thermal Management," SAE 23rd International Conference on Environmental Systems, Colorado Springs, Colorado.

[3] Puterbaugh, R. L., Brown, J., and Battelle, R., 2011, "Integrated Engine/Thermal Architecture Model Interface Development," SAE Technical Paper 2011-01-2585, doi: 10.4271/2011-01-2585.

[4] Dooley, M., Lui, N., Newman, R., and Lui, C., 2014, "Aircraft Thermal Management –Heat Sink Challenge," SAE Technical Paper 2014-01-2193, doi: 10.4271/2014-01-2193.

[5] Puterbaugh, R. L., Brown, J., and Battelle, R., 2012, "Impact of Heat Exchanger Location on Engine Performance," SAE Technical Paper 2012-01-2168, doi: 10.4271/2012-01-2168.

[6] Adeniyi, A.A., Morvan, H. P., and Simmons, K. A., 2015, "A Multiphase Computational Study of Oil-Air Flow within the Bearing Sector of Aeroengines," Proc. Of ASME Turbo Expo 2015, GT2015-43496, Montreal, Canada.

[7] Hannon, W. M., 2015, "Rolling-Element Bearing Heat Transfer Part I – Analytic Model," ASME Journal of Tribology, Vol. 137, July 2015.

[8] Gupta, P. K., 1984, "Advanced Dynamics of Rolling Elements," Springer-Verlag, New York, NY., Chap. 5 & 6.

[9] Kannel, J. W., and Walowit, J.W., 1971, "Simplified Analysis of Tractions Between Rolling-Sliding Elastohydrodynamic Contacts," ASME Journal of Lubrication Technology, Vol. 93, pp. 39-46.

[10] Johnson, K. L., and Tevaarwerk, J. L., 1977, "Shear Behvior of Elastohydrodynamic Oil Films," Proc. Royal Society, London, Series A356, pp. 215-236.

[11] Bair, S., and Winer, W. O., 1979, "A Rheological Model for Elastohydrodynamic Contacts Based on Primary Laboratory Data," Journal of Lubrication Technology, ASME Trans., Vol. 101, pp. 258-265, 1979.

[12] Gupta, P. K., Cheng, H. S., and Forster, N. H., 1992, "Visco-Elastic Effects in MIL-L-7808 Type Lubricant, Part I: Analytical Formulation," Tribol. Trans. Vol. 35, pp. 269-274.

[13] Bair, S., 2006, "Reference Liquids for Quantitative Elastohydrodynamics: Selection and Rheological Characterization," Tribology Letters, Vol 22, #2, pp 197-206, May.

[14] Bair, S., 2014, "Shear-Thinning at Pressures above Ambient", Presented at 2014 STLE Annual Meeting, Orlando, FL May18-22, 2014.

[15] Crecelius, W. J., and Pirvics, J., 1976, "Computer Program Operation Manual on SHABERTH a Computer Program for the Analysis of the Steady State and Transient Thermal Performance of Shaft-Bearing Systems," Report, Air Force AFAPL-TR-76-90.

[16] Woods, C. M., 1990, "Modification of the SHABERTH Bearing Code to Incorporate RP-1 and a Discussion of the Traction Model," NASA Technical Paper 3017.

[17] Gupta, P. K., 2011, "Current Status of and Future Innovation in Rolling Bearing Modeling," Tribol. Trans. Vol. 54, #3, pp. 394-403.

[18] Rumbarger, J. H., Filetti, E. G., and Gubernick, D., 1973, "Gas Turbine Engine Main Shaft Roller Bearing System Analysis," ASME Journal of Lubrication Technology, Vol. 95, pp 401-416.

[19] Forster, N.H., Svendsen, V.R., Givan, G.D., Thompson, K. L., Dao, N.H., and Nicholson, B. D., 2011, "Parametric Testing and Heat Generation Modeling of 133-mm Bore Ball Bearings: Part I—Results with Metal Rolling Elements," Tribol. Trans. Vol. 54, #2, pp. 315-324.

[20] Hamrock, B. J., and Dowson, D., 1981, "Ball Bearing Lubrication: Elastohydrodynamics of Elliptical Contacts," John Wiley and Sons, Hoboken, NJ.

[21] Cheng, H. S., and Sternlicht, B., 1965, "A Numerical Solution for the Pressure, Temperature and Film Thickness Between Two Infinitely Long, Lubricated Rolling and Sliding Cylinders under Heavy Loads," ASME Journal of Basic Engineering, Vol. 87, pp. 695-707.

[22] Cheng, H. S., 1970, "A Numerical Solution of the Elastohydrodynamic Film Thickness in an Elliptical Contact," ASME Journal of Lubrication Technology, Vol. 92, pp. 155-162.

[23] Wilson, W. R. D., and Sheu, S., 1983, "Effect of Inlet Shear Heating Due to Sliding on Elastohydrodynamic Film Thickness," ASME Journal of Lubrication Technology, Vol. 105, pp 187-188.

[24] Wright, W. A., 1969, "An Improved Viscosity-Temperature Chart for Hydrocarbons," Journal of Materials, 4(1), pp. 19-27.

[25] Parker, R. J., 1984, "Comparison of Predicted and Experimental Thermal Performance of Angular Contact Ball Bearings," Technical Paper, NASA TP-2275.

[26] Pinel, S. I., Signer, H. R., and Zaretsky, E. V., 1998, "Design and Operating Characteristics of High-Speed, Small-Bore, Angular-Contact Ball Bearings," Technical Memorandum, NASA TM-1998-206981.